Asian Journal of Chemistry; Vol. 27, No. 7 (2015), 2598-2602

ASIAN JOURNAL OF CHEMISTRY

http://dx.doi.org/10.14233/ajchem.2015.18428

Cyclic Microwave-Assisted Sol-Gel Process of $KGd(MoO_4)_2:Er^{3+}/Yb^{3+}$ Phosphors and Upconversion of their Photoluminescence Properties

CHANG SUNG LIM

Department of Advanced Materials Science and Engineering, Hanseo University, Seosan 356-706, Republic of Korea

Corresponding author: Tel/Fax: +82 41 6601445; E-mail: cslim@hanseo.ac.kr

Received: 12 July 2014; *Accepted*: 17 November 2014; *Published online*: 30 March 2015; AJC-17087

$KGd_{1-x}(MoO_4)_2:Er^{3+}/Yb^3$ phosphors with doping concentrations of Er^{3+} and Yb^{3+} ($x = Er^{3+} + Yb^{3+}$, $Er^{3+} = 0.05, 0.1, 0.2$ and $Yb^{3+} = 0.2, 0.45$) Er^{3+} and Yb^{3+} ($Er^{3+} = 0.05, 0.1, 0.2$ and $Yb^{3+} = 0.2, 0.45$) were successfully synthesized by a cyclic microwave-assisted sol-gel process and the upconversion and spectroscopic properties were investigated. Well-crystallized particles showed a fine and homogeneous morphology with particle sizes of 2-8 μm. Under excitation at 980 nm, $KGd_{0.7}(MoO_4)_2:Er_{0.1}Yb_{0.2}$ and $KGd_{0.5}(MoO_4)_2:Er_{0.05}Yb_{0.45}$ particles exhibited a strong 525 nm emission band, a weak 550 nm emission band in the green region and a very weak 655 nm emission band in the red region. The Raman spectra of $KGd_{0.8}(MoO_4)_2:Er_{0.2}$, $KGd_{0.7}(MoO_4)_2:Er_{0.1}Yb_{0.2}$ and $KGd_{0.5}(MoO_4)_2:Er_{0.05}Yb_{0.45}$ particles indicated the domination of strong peaks at higher frequencies (1050, 1065, 1125, 1185, 1284, 1350 and 1420 cm^{-1}) and at lower frequencies (258, 388, 462, 558, 630 and 674 cm^{-1}).

Keywords: Upconversion photoluminescence, Microwave-assisted sol-gel process, Raman spectroscopy.

INTRODUCTION

Photoluminescence particles have evolved in their applications, such as fluorescent lamps, cathode ray tubes, solid-state laser, amplifiers for fiber optics communication and new optoelectronic devices, which show high luminescence quantum yields, since usually more than one metastable excited state exists, multiple emissions are observed[1,2]. Rare earth activated upconversion (UC) particles can convert near infrared radiation of low energy into visible radiation of high energy. Recently, the synthesis and the luminescence properties of upconversion particles have attracted considerable interest since they are considered as potentially active components in new optoelectronic devices and luminescent labels for imaging and biodetection assays, which overcome the current limitations in traditional photoluminescence materials[3]. The double molybdate compounds of $MR_2(MoO_4)_4$ (M: bivalent alkaline earth metal ion, R: trivalent rare earth ion) belong to a group of double alkaline earth lanthanide molybdates. With the decrease in the ionic radius of alkaline earth metal ions ($R_{Ca} < R_{Sr} < R_{Ba}$; R = ionic radius), it is possible for the structure of $MR_2(MoO_4)_4$ to be transformed to a highly disordered tetragonal Scheelite structure from the monoclinic structure. It is possible for the trivalent rare earth ions in the disordered tetragonal-phase to be partially substituted by Er^{3+} and Yb^{3+} ions, these ions are effectively doped into the crystal lattices of the tetragonal phase due to the similar radii of the trivalent rare earth ions in R^{3+}, this results in the excellent upconversion photoluminescence properties[4-6]. Among rare earth ions, the Er^{3+} ion is suitable for converting infrared to visible light through the upconversion process due to its appropriate electronic energy level configuration. The co-doped Yb^{3+} ion and Er^{3+} ion can remarkably enhance the upconversion efficiency for the shift from infrared to visible light due to the efficiency of the energy transfer from Yb^{3+} to Er^{3+}. The Yb^{3+} ion, as a sensitizer, can be effectively excited by an incident light source energy. This energy is transferred to the activator from which radiation can be emitted. The Er^{3+} ion activator is the luminescence center of the upconversion particles, while the sensitizer enhances the upconversion luminescence efficiency[7-9].

Recently, rare earth activated $MR_2(MoO_4)_4$ (M = Ba, Sr, Ca; R = La, Gd, Y) has attracted great attention because of the its spectroscopic characteristics and excellent upconversion photoluminescence properties. Several processes have been developed to prepare these rare-earth-doped double molybdates, including solid-state reactions[9-14], co-precipitation[15,16], the sol-gel method[4-7], the hydrothermal method[17,18], the Pechini method[19,20], organic gel-thermal decomposition[21] and the microwave-assisted hydrothermal method[22]. For practical application of upconversion photoluminescence in products such as lasers, three-dimensional displays, light-emitting devices and biological detectors, features such as the homogeneous

upconversion particle size distribution and morphology need to be well defined. Usually, double molybdates are prepared by a solid-state method that requires high temperatures, a lengthy heating process and subsequent grinding, this results in a loss of the emission intensity and an increase in cost. The sol-gel process provides some advantages over the conventional solid-state method, including good homogeneity, low calcination temperature, small particle size and narrow particle size distribution optimal for good luminescent characteristics. However, the sol-gel process has a disadvantage in that it takes a long time for gelation. Compared with the usual methods, microwave synthesis has the advantages of a very short reaction time, small-size particles, narrow particle size distribution and high purity of final polycrystalline samples. Microwave heating is delivered to the material surface by radiant and/or convection heating, which is transferred to the bulk of the material *via* conduction[23,24]. A cyclic microwave-modified sol-gel process is a cost-effective method that provides high homogeneity and is easy to scale-up and it is emerging as a viable alternative approach for the quick synthesis of high-quality luminescent materials.

In this study, $KGd_{1-x}(MoO_4)_2:Er^{3+}/Yb^{3+}$ phosphors with doping concentrations of Er^{3+} and Yb^{3+} ($x = Er^{3+} + Yb^{3+}$, Er^{3+} = 0.05, 0.1, 0.2 and Yb^{3+} = 0.2, 0.45) phosphors were prepared by the cyclic microwave-assisted sol-gel process followed by heat treatment. The synthesized particles were characterized by X-ray diffraction (XRD), scanning electron microscopy (SEM) and energy-dispersive X-ray spectroscopy (EDS). The optical properties were examined comparatively using photoluminescence (PL) emission and Raman spectroscopy.

EXPERIMENTAL

Appropriate stoichiometric amounts of KNO_3 (99 %, Sigma-Aldrich, USA), $Gd(NO_3)_3·6H_2O$ (99 %, Sigma-Aldrich, USA), $(NH_4)_6Mo_7O_{24}·4H_2O$ (99 %, Alfa Aesar, USA), Er-$(NO_3)_3·5H_2O$ (99.9 %, Sigma-Aldrich, USA), $Yb(NO_3)_3·5H_2O$ (99.9 %, Sigma-Aldrich, USA), citric acid (99.5 %, Daejung Chemicals, Korea), NH_4OH (A.R.), ethylene glycol (A.R.) and distilled water were used to prepare $KGd(MoO_4)_2$, $KGd_{0.8}(Mo-O_4)_2:Er_{0.2}$, $KGd_{0.7}(MoO_4)_2:Er_{0.1}Yb_{0.2}$ and $KGd_{0.5}(MoO_4)_2:Er_{0.05}Yb_{0.45}$ compounds with doping concentrations of Er^{3+} and Yb^{3+} (Er^{3+} = 0.05, 0.1, 0.2 and Yb^{3+} = 0.2, 0.45). To prepare $KGd(MoO_4)_2$, 0.4 mol % KNO_3 and 0.4 mol % $(NH_4)_6Mo_7O_{24}·4H_2O$ were dissolved in 20 mL of ethylene glycol and 80 mL of 5 M NH_4OH under vigorous stirring and heating. Subsequently, 0.4 mol % $Gd(NO_3)_3·6H_2O$ and citric acid (with a molar ratio of citric acid to total metal ions of 2:1) were dissolved in 100 mL of distilled water under vigorous stirring and heating. Then, the solutions were mixed together under vigorous stirring and heating at 80-100 °C. At the end, highly transparent solutions were obtained and adjusted to pH = 7-8 by the addition of 8 M NH_4OH or citric acid. In order to prepare $KGd_{0.8}(MoO_4)_2:Er_{0.2}$, the mixture of 0.32 mol % $Gd(NO_3)_3·6H_2O$ with 0.08 mol % $Er(NO_3)_3·5H_2O$ was used for the formation of the rare earth solution. In order to prepare $KGd_{0.7}(MoO_4)_2:Er_{0.1}Yb_{0.2}$, the mixture of 0.28 mol % $Gd(NO_3)_3·6H_2O$ with 0.04 mol % $Er(NO_3)_3·5H_2O$ and 0.08 mol % $Yb(NO_3)_3·5H_2O$ was used for the creation of the rare earth solution. In order to prepare $KGd_{0.5}(MoO_4)_2:Er_{0.05}Yb_{0.45}$, the rare earth containing solution was generated using 0.2 mol % $Gd(NO_3)_3·6H_2O$ with 0.02 mol % $Er(NO_3)_3·5H_2O$ and 0.18 mol % $Yb(NO_3)_3·5H_2O$.

The transparent solutions were placed into a microwave oven operating at a frequency of 2.45 GHz with a maximum output-power of 1250 W for 0.5 h. The working cycle of the microwave reaction was controlled precisely using a regime of 40 s on and 20 s off for 15 min, followed by further treatment of 30 s on and 30 s off for 15 min. The ethylene glycol was evaporated slowly at its boiling point. Ethylene glycol is a polar solvent at its boiling point of 197 °C, this solvent is a good candidate for the microwave process. If ethylene glycol is used as the solvent, the reactions proceed at the boiling point temperature. When microwave radiation is supplied to the ethylene-glycol-based solution, the components dissolved in the ethylene glycol can couple. The charged particles vibrate in the electric field interdependently when a large amount of microwave radiation is supplied to the ethylene glycol. The samples were treated with ultrasonic radiation for 10 min to produce a light yellow transparent sol. After this, the light yellow transparent sols were dried at 120 °C in a dry oven to obtain black dried gels. The black dried gels were grinded and heat-treated at 900 °C for 16 h with 100 °C intervals between 600-900 °C. Finally, white particles were obtained for $KGd(MoO_4)_2$ and pink particles for $KGd_{0.8}(MoO_4)_2:Er_{0.2}$, $KGd_{0.7}(MoO_4)_2:Er_{0.1}Yb_{0.2}$ and $KGd_{0.5}(MoO_4)_2:Er_{0.05}Yb_{0.45}$ compositions.

The phase composition of the synthesized particles was identified using XRD (D/MAX 2200, Rigaku, Japan). The microstructure and surface morphology of the $KGd(MoO_4)_2$, $KGd_{0.8}(MoO_4)_2:Er_{0.2}$, $KGd_{0.7}(MoO_4)_2:Er_{0.1}Yb_{0.2}$ and $KGd_{0.5}(MoO_4)_2:Er_{0.05}Yb_{0.45}$ particles were observed using SEM/EDS (JSM-5600, JEOL, Japan). The photoluminescence spectra were recorded using a spectrophotometer (Perkin Elmer LS55, UK) at room temperature. Raman spectroscopy measurements were performed using a LabRam Aramis (Horiba Jobin-Yvon, France). The 514.5 nm line of an Ar ion laser was used as the excitation source and the power on the samples was kept at 0.5 mW.

RESULTS AND DISCUSSION

Fig. 1 shows the XRD patterns of the (a) JCPDS 32-0785 data of $KGd(MoO_4)_2$, the synthesized (b) $KGd(MoO_4)_2$, (c) $KGd_{0.8}(MoO_4)_2:Er_{0.2}$, (d) $KGd_{0.7}(MoO_4)_2:Er_{0.1}Yb_{0.2}$ and (e) $KGd_{0.5}(MoO_4)_2:Er_{0.05}Yb_{0.45}$ particles. The crystal structures of (a) $KGd(MoO_4)_2$, (b) $KGd_{0.8}(MoO_4)_2:Er_{0.2}$ particles were assigned to the crystallographic data of $KGd(MoO_4)_2$ (JCPDS 32-0785) belonging to orthorhombic system. However, with increasing of the Yb^{3+} ions, the crystal structures of (c) $KGd_{0.7}(MoO_4)_2:Er_{0.1}Yb_{0.2}$ and (d) $KGd_{0.5}(MoO_4)_2:Er_{0.05}Yb_{0.45}$ showed another phase of $KYb(MoO_4)_2$ (JCPDS 50-1762) belonging to orthorhombic system[20]. It is assumed that the doping amount of Er^{3+}/Yb^{3+} has a great effect on the crystalline cell volume of the $KGd(MoO_4)_2$, which was transformed to the $KYb(MoO_4)_2$ structure, because of the different ionic sizes and energy band gaps. This means that the obtained samples possess a partial substitution of Gd^{3+} by Er^{3+} and Yb^{3+} ions and the ions are effectively doped into crystal lattices of the $KGd(MoO_4)_2$ phase due to the similar radii of Gd^{3+}, Er^{3+} and Yb^{3+}. Post

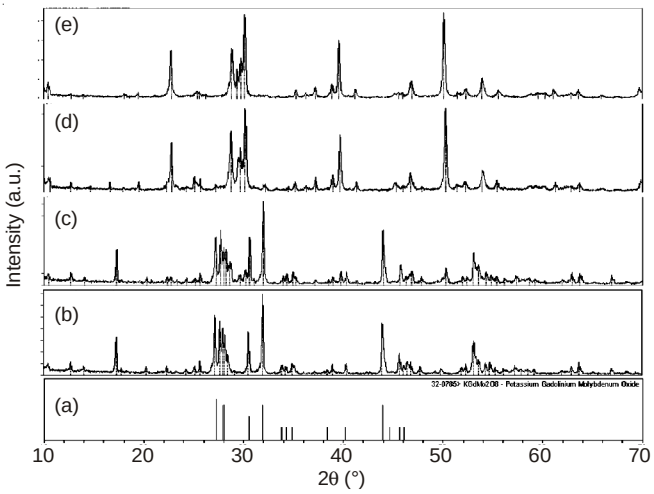

Fig. 1. X-ray diffraction patterns of (a) JCPDS 32-0785 data of $KGd(MoO_4)_2$, the synthesized (b) $KGd(MoO_4)_2$, (c) $KGd_{0.8}(MoO_4)_2$: $Er_{0.2}$, (d) $KGd_{0.7}(MoO_4)_2$:$Er_{0.1}Yb_{0.2}$ and (e) $KGd_{0.5}(MoO_4)_2$:$Er_{0.05}Yb_{0.45}$ particles

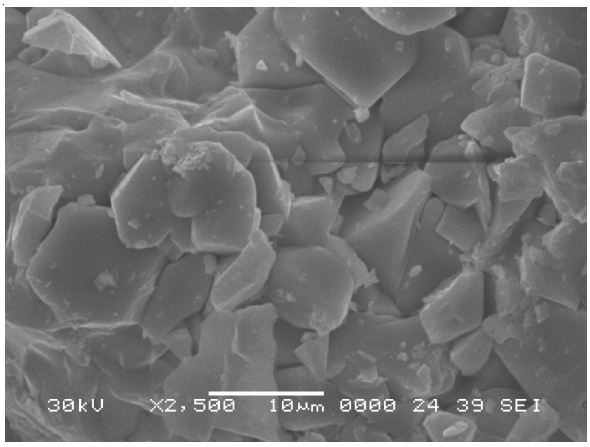

Fig. 2. Scanning electron microscopy images of the synthesized (a) $KGd(MoO_4)_2$, (b) $KGd_{0.8}(MoO_4)_2$:$Er_{0.2}$, (c) $KGd_{0.7}(MoO_4)_2$:$Er_{0.1}Yb_{0.2}$ and (e) $KGd_{0.5}(MoO_4)_2$:$Er_{0.05}Yb_{0.45}$ particles

heat-treatment plays an important role in a well-defined crystallized morphology. To achieve a well-defined crystalline morphology, $KGd(MoO_4)_2$, $KGd_{0.8}(MoO_4)_2$:$Er_{0.2}$, $KGd_{0.7}(MoO_4)_2$:$Er_{0.1}Yb_{0.2}$ and $KGd_{0.5}(MoO_4)_2$:$Er_{0.05}Yb_{0.45}$ phases need to be heat treated at 900 °C for 16 h.

Fig. 2 shows SEM images of the synthesized $KGd_{0.5}(MoO_4)_2$:$Er_{0.05}Yb_{0.45}$ particles. The as-synthesized samples are well crystallized with a fine and homogeneous morphology and particle size of 2-10 µm. This suggests that the cyclic microwave-assisted sol-gel route is suitable for the growth of $KGd_{1-x}(MoO_4)_2$:Er^{3+}/Yb^{3+} crystallites. Fig. 3 shows the energy-dispersive X-ray spectroscopy patterns of the synthesized (a) $KGd_{0.8}(MoO_4)_2$:$Er_{0.2}$ and (b) $KGd_{0.5}(MoO_4)_2$:$Er_{0.05}Yb_{0.45}$ particles and quantitative compositions of (c) $KGd_{0.8}(MoO_4)_2$:$Er_{0.2}$ and (d) $KGd_{0.5}(MoO_4)_2$:$Er_{0.05}Yb_{0.45}$ particles. The EDS pattern shows that the (a) $KGd_{0.8}(MoO_4)_2$:$Er_{0.2}$ and (b) $KGd_{0.5}(MoO_4)_2$:$Er_{0.05}Yb_{0.45}$ particles are composed of K, Gd, Mo, O and Er for $KGd_{0.8}(MoO_4)_2$:$Er_{0.2}$ and K, Gd, Mo, O, Er and Yb for $KGd_{0.5}(MoO_4)_2$:$Er_{0.05}Yb_{0.45}$ particles. The quantitative compositions of (c) and (d) are in good relation with nominal compositions of the particles. The relation of K, Gd, Mo, O, Er and Yb components exhibit that $KGd_{0.8}(MoO_4)_2$:$Er_{0.2}$ and $KGd_{0.5}(MoO_4)_2$:$Er_{0.05}Yb_{0.45}$ particles can be successfully synthesized using the cyclic microwave-assisted sol-gel process. The cyclic microwave-assisted sol-gel process of double molybdates provides the energy to synthesize the bulk of the material uniformly, so that fine particles with controlled morphology can be fabricated in a short time period. The

(a)

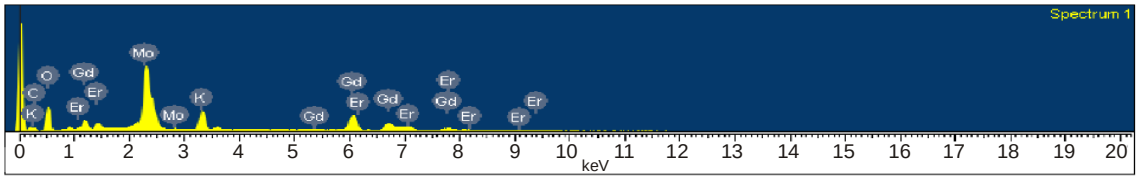

(b)

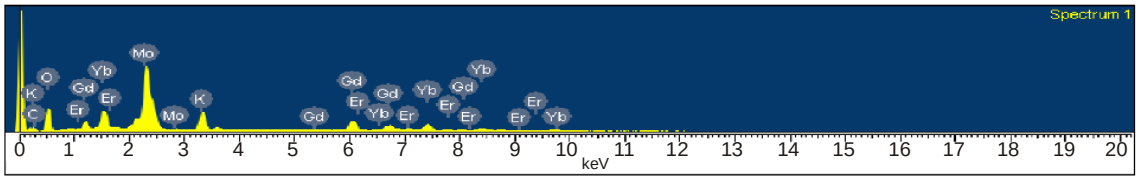

(c)

Spectrum	In stats.	C	O	K	Mo	Gd	Er	Total
Spectrum 1	Yes	7.63	35.51	4.56	29.69	18.27	4.34	100.00
Spectrum 2	Yes	8.68	35.31	4.42	29.57	17.62	4.40	100.00
Spectrum 3	Yes	5.17	36.16	4.87	30.59	18.31	4.91	100.00
Spectrum 4	Yes	6.07	36.64	4.68	30.28	17.65	4.74	100.00
Mean		6.87	35.90	4.63	30.03	17.96	4.60	100.00
Std. deviation		1.58	0.61	0.19	0.48	0.38	0.27	
Max.		8.68	36.64	4.87	30.59	18.31	4.91	
Min.		5.17	35.31	4.42	29.57	17.62	4.34	

(d)

Spectrum	In stats.	C	O	K	Mo	Gd	Er	Yb	Total
Spectrum 1	Yes	8.83	33.48	4.36	29.09	10.88	0.44	12.92	100.00
Spectrum 2	Yes	4.81	34.25	4.71	31.02	11.05	0.33	13.83	100.00
Spectrum 3	Yes	1.50	35.54	4.79	31.64	11.68	1.11	13.75	100.00
Spectrum 4	Yes	4.42	34.95	4.52	31.46	11.50	0.70	12.45	100.00
Mean		4.89	43.55	4.60	30.80	11.28	0.64	13.24	100.00
Std. deviation		3.02	0.89	0.20	1.17	0.37	0.34	0.66	
Max.		8.83	35.54	4.79	31.64	11.68	1.11	13.83	
Min.		1.50	33.48	4.36	29.09	10.88	0.33	12.45	

Fig. 3. Energy-dispersive X-ray spectroscopy patterns of the synthesized (a) $KGd_{0.7}(MoO_4)_2$:$Er_{0.1}Yb_{0.2}$ and (b) $KGd_{0.5}(MoO_4)_2$:$Er_{0.05}Yb_{0.45}$ particles, and quantitative compositions of (c) $KGd_{0.7}(MoO_4)_2$: $Er_{0.1}Yb_{0.2}$ and (d) $KGd_{0.5}(MoO_4)_2$:$Er_{0.05}Yb_{0.45}$ particles

method is a cost-effective way to provide highly homogeneous products and is easy to scale-up, it is a viable alternative for the rapid synthesis of upconversion particles.

Fig. 4 shows the upconversion photoluminescence emission spectra of the as-prepared (a) $KGd(MoO_4)_2$, (b) $KGd_{0.8}(MoO_4)_2:Er_{0.2}$, (c) $KGd_{0.7}(MoO_4)_2:Er_{0.1}Yb_{0.2}$ and (d) $KGd_{0.5}(MoO_4)_2:Er_{0.05}Yb_{0.45}$ particles excited under 980 nm at room temperature. The upconversion intensities of (c) $KGd_{0.7}(MoO_4)_2:Er_{0.1}Yb_{0.2}$ and (d) $KGd_{0.5}(MoO_4)_2:Er_{0.05}Yb_{0.45}$ particles exhibited a strong 525 nm emission band, a weak 550 nm emission band in the green region and a very weak 655 nm emission band in the red region. The strong 525 nm emission band and the weak 550 nm emission band in the green region correspond to the $^2H_{11/2} \rightarrow {}^4I_{15/2}$ and $^4S_{3/2} \rightarrow {}^4I_{15/2}$ transitions, respectively, while the weak emission band at 655 nm in the red region corresponds to the $^4F_{9/2} \rightarrow {}^4I_{15/2}$ transition. The upconversion intensities of (a) $KGd(MoO_4)_2$ and (b) $KGd_{0.8}(MoO_4)_2:Er_{0.2}$ were not detected. The upconversion intensity of (d) $KGd_{0.5}(MoO_4)_2:Er_{0.05}Yb_{0.45}$ is much higher than that of (c) $KGd_{0.7}(MoO_4)_2:Er_{0.1}Yb_{0.2}$ particles. Similar results are also observed from Er^{3+}/Yb^{3+} co-doped in other host matrices, which are assigned to the upconversion emission spectra with the green emission intensity ($^2H_{11/2} \rightarrow {}^4I_{15/2}$ and $^4S_{3/2} \rightarrow {}^4I_{15/2}$ transitions) and the red emission intensity ($^4F_{9/2} \rightarrow {}^4I_{15/2}$ transition)[10,25-28]. The upconversion process is a proven method for generating visible light from near infrared (NIR) radiation. Upconversion is a nonlinear optical process in which excitation of the lower electronic levels with low-energy radiation (NIR light) results in higher energy emission (visible or ultraviolet light) at higher electronic levels; thus, it is ascribed as an anti-stockes mechanism. This process requires the absorption of two or more photons to produce sufficient energy for upconversion emission. The doping amounts of Er^{3+}/Yb^{3+} had a great effect on the morphological features of the particles and their upconversion fluorescence intensity. The Yb^{3+} ion sensitizer can be effectively excited by the energy of an incident light source, this energy is transferred to the activator where radiation can be emitted. The Er^{3+} ion activator is the luminescence center for these upconversion particles and the sensitizer enhances the upconversion luminescence efficiency. The much higher intensity of the $^2H_{11/2} \rightarrow {}^4I_{15/2}$ transition in comparison with the $^4S_{3/2} \rightarrow {}^4I_{15/2}$ transition may be induced by the concentration quenching effect due to the energy transfer between the nearest Er^{3+} and Yb^{3+} ions and the interactions between doping ions in the $KGd_{1-x}(MoO_4)_2:Er^{3+}/Yb^{3+}$ host matrix[10,25]. This means that the green band $^2H_{11/2} \rightarrow {}^4I_{15/2}$ transitions are assumed to be more easily quenched than the $^4S_{3/2} \rightarrow {}^4I_{15/2}$ transition by non-radiative relaxation in the case of the host matrix.

Fig. 5 shows the Raman spectra of the synthesized (a) $KGd(MoO_4)_2$(KGM), (b) $KGd_{0.8}(MoO_4)_2:Er_{0.2}$(KGM:Er), (c) $KGd_{0.7}(MoO_4)_2:Er_{0.1}Yb_{0.2}$(KGM:ErYb) and (d) $KGd_{0.5}(MoO_4)_2:Er_{0.05}Yb_{0.45}$(KGM:ErYb#) particles excited by the 514.5 nm line of an Ar ion laser at 0.5 mW. The internal modes for the (a) $KGd(MoO_4)_2$(KGM) particles were detected at 320, 762, 820, 862 and 954 cm^{-1}, respectively. The well-resolved sharp peaks for the $KGd(MoO_4)_2$(KGM) particles indicate a high crystallinity state of the synthesized particles. The internal vibration mode frequencies are dependent on the lattice parameters and the degree of the partially covalent bond between the cation and molecular ionic group $[MoO_4]^{2-}$. The Raman spectra of the (b) $KGd_{0.8}(MoO_4)_2:Er_{0.2}$(KGM:Er), (c) $KGd_{0.7}(MoO_4)_2:Er_{0.1}Yb_{0.2}$(KGM:ErYb) and (d) $KGd_{0.5}(MoO_4)_2:Er_{0.05}Yb_{0.45}$(KGM:ErYb#) particles indicate the domination of strong peaks at higher frequencies (1050, 1065, 1125, 1185, 1284, 1350 and 1420 cm^{-1}) and at lower frequencies (258, 388, 462, 558, 630 and 674 cm^{-1}). The Raman spectra of (b) $KGd_{0.5}(MoO_4)_2:Er_{0.05}Yb_{0.45}$(KGM:Er), (c) $KGd_{0.7}(MoO_4)_2:Er_{0.1}Yb_{0.2}$(KGM:ErYb) and (d) $KGd_{0.5}(MoO_4)_2:Er_{0.05}Yb_{0.45}$(KGM:ErYb#) particles prove that the doping ions can influence the structure of the host materials. The combination of a heavy metal cation and the large inter-ionic distance for Er^{3+} and Yb^{3+} substitutions in Gd^{3+} sites in the lattice result in a low probability of upconversion and phonon-splitting relaxation in $KGd_{1-x}(MoO_4)_2:Er^{3+}/Yb^{3+}$ crystals. It may be that these very strong and strange effects are generated by the

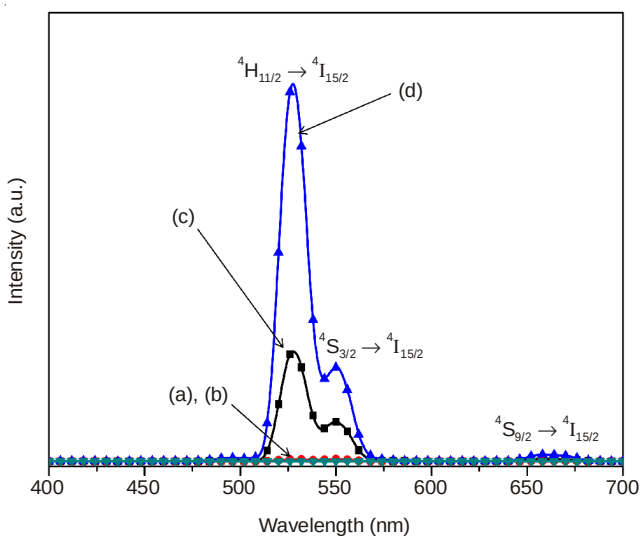

Fig. 4. Upconversion photoluminescence emission spectra of (a) $KGd(MoO_4)_2$, (b) $KGd_{0.8}(MoO_4)_2:Er_{0.2}$, (c) $KGd_{0.7}(MoO_4)_2:Er_{0.1}Yb_{0.2}$ and (e) $KGd_{0.5}(MoO_4)_2:Er_{0.05}Yb_{0.45}$ particles excited under 980 nm at room temperature

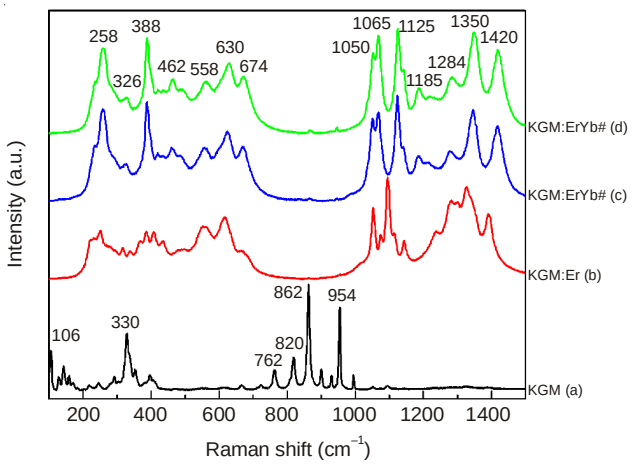

Fig. 5. Raman spectra of the synthesized (a) $KGd(MoO_4)_2$(KGM), (b) $KGd_{0.5}(MoO_4)_2:Er_{0.05}Yb_{0.45}$(KGM:Er), (c) $KGd_{0.7}(MoO_4)_2:Er_{0.1}Yb_{0.2}$ (KGM:ErYb) and (d) $KGd_{0.5}(MoO_4)_2:Er_{0.05}Yb_{0.45}$(KGM:ErYb#) particles excited by the 514.5 nm line of an Ar ion laser at 0.5 mW

disorder of the $[MoO_4]^{2-}$ groups with the incorporation of the Er^{3+} and Yb^{3+} elements into the crystal lattice or by a new phase formation.

Conclusion

The upconversion $KGd_{1-x}(MoO_4)_2:Er^{3+}/Yb^{3+}$ phosphors with doping concentrations of Er^{3+} and Yb^{3+} ($x = Er^{3+} + Yb^{3+}$, $Er^{3+} = 0.05$, 0.1, 0.2 and $Yb^{3+} = 0.2$, 0.45) were successfully synthesized by the cyclic microwave-assisted sol-gel process. Well-crystallized particles formed after heat-treatment at 900 °C for 16 h showed a fine and homogeneous morphology with particle sizes of 2-8 μm. Under excitation at 980 nm, the upconversion intensities of $KGd_{0.7}(MoO_4)_2:Er_{0.1}Yb_{0.2}$ and $KGd_{0.5}(MoO_4)_2:Er_{0.05}Yb_{0.45}$ particles exhibited a strong 525 nm emission band and a weak 550 nm emission band in the green region, which were assigned to the $^2H_{11/2} \rightarrow {}^4I_{15/2}$ and $^4S_{3/2} \rightarrow {}^4I_{15/2}$ transitions, respectively, while a weak emission band at 655 nm in the red region was assigned to the $^4F_{9/2} \rightarrow {}^4I_{15/2}$ transition. The upconversion intensity of $KGd_{0.5}(MoO_4)_2:Er_{0.05}Yb_{0.45}$ particles was much higher than that of the $KGd_{0.7}(MoO_4)_2:Er_{0.1}Yb_{0.2}$ particles. The Raman spectra of the $KGd_{0.8}(MoO_4)_2:Er_{0.2}$, $KGd_{0.7}(MoO_4)_2:Er_{0.1}Yb_{0.2}$ and $KGd_{0.5}(MoO_4)_2:Er_{0.05}Yb_{0.45}$ particles indicate the domination of strong peaks at higher frequencies (1050, 1065, 1125, 1185, 1284, 1350 and 1420 cm^{-1}) and at lower frequencies (258, 388, 462, 558, 630 and 674 cm^{-1}) induced by the disorder of the $[MoO_4]^{2-}$ groups with the incorporation of the Er^{3+} and Yb^{3+} elements into the crystal lattice or by a new phase formation.

ACKNOWLEDGEMENTS

This study was supported by the Basic Science Research Program through the National Research Foundation of Korea (NRF) funded the Ministry of Science, ICT & Future Planning (2014-046024).

REFERENCES

1. M. Lin, Y. Zhao, S.Q. Wang, M. Liu, Z.F. Duan, Y.M. Chen, F. Li, F. Xu and T.J. Lu, *Bio. Adv*., **30**, 1551 (2012).
2. M. Wang, G. Abbineni, A. Clevenger, C. Mao and S. Xu, *Nanomedicine*, **7**, 710 (2011).
3. A. Shalav, B.S. Richards and M.A. Green, *Sol. Energy Mater. Sol. Cells*, **91**, 829 (2007).
4. C. Guo, H.K. Yang and J.H. Jeong, *J. Lumin*., **130**, 1390 (2010).
5. J. Liao, D. Zhou, B. Yang, R. Liu, Q. Zhang and Q. Zhou, *J. Lumin*., **134**, 533 (2013).
6. J. Sun, J. Xian and H. Du, *J. Phys. Chem. Solids*, **72**, 207 (2011).
7. T. Li, C. Guo, Y. Wu, L. Li and J.H. Jeong, *J. Alloys Comp*., **540**, 107 (2012).
8. M. Nazarov and D.Y. Noh, *J. Rare Earths*, **28**, 1 (2010).
9. J. Sun, W. Zhang, W. Zhang and H. Du, *Mater. Res. Bull*., **47**, 786 (2012).
10. H. Du, Y. Lan, Z. Xia and J. Sun, *Mater. Res. Bull*., **44**, 1660 (2009).
11. Z. Wang, H. Liang, M. Gong and Q. Su, *J. Alloys Comp*., **432**, 308 (2007).
12. M. Haque and D.K. Kim, *Mater. Lett*., **63**, 793 (2009).
13. C. Zhao, X. Yin, F. Huang and Y. Hang, *J. Solid State Chem*., **184**, 3190 (2011).
14. L. Qin, Y. Huang, T. Tsuboi and H.J. Seo, *Mater. Res. Bull*., **47**, 4498 (2012).
15. Y.L. Yang, X.M. Li, W.L. Feng, W.L. Li and C.Y. Tao, *J. Alloys Comp*., **505**, 555 (2010).
16. Y. Tian, B. Chen, B. Tian, R. Hua, J. Sun, L. Cheng, H. Zhong, X. Li, J. Zhang, Y. Zheng, T. Yu, L. Huang and Q. Meng, *J. Alloys Comp*., **509**, 6096 (2011).
17. Y. Huang, L. Zhou, L. Yang and Z. Tang, *Opt. Mater*., **33**, 777 (2011).
18. Y. Tian, B. Chen, B. Tian, J. Sun, X. Li, J. Zhang, L. Cheng, H. Zhong, H. Zhong, Q. Meng and R. Hua, *Physica B*, **407**, 2556 (2012).
19. Z. Wang, H. Liang, L. Zhou, J. Wang, M. Gong and Q. Su, *J. Lumin*., **128**, 147 (2008).
20. Q. Chen, L. Qin, Z. Feng, R. Ge, X. Zhao and H. Xu, *J. Rare Earths*, **29**, 843 (2011).
21. X. Shen, L. Li, F. He, X. Meng and F. Song, *Mater. Chem. Phys*., **132**, 471 (2012).
22. J. Zhang, X. Wang, X. Zhang, X. Zhao, X. Liu and L. Peng, *Inorg. Chem. Commun*., **14**, 1723 (2011).
23. S. Das, A.K. Mukhopadhyay, S. Datta and D. Basu, Bull. Mater. Sci., 32, 1 (2009).
24. T. Thongtem, A. Phuruangrat and S. Thongtem, *J. Nanopart. Res*., **12**, 2287 (2010).
25. C.S. Lim, *Mater. Res. Bull*., **48**, 3805 (2013).
26. W. Lu, L. Cheng, J. Sun, H. Zhong, X. Li, Y. Tian, J. Wan, Y. Zheng, L. Huang, T. Yu, H. Yu and B. Chen, *Physica B*, **405**, 3284 (2010).
27. J. Sun, J. Xian, X. Zhang and H. Du, *J. Rare Earths*, **29**, 32 (2011).
28. Q. Sun, X. Chen, Z. Liu, F. Wang, Z. Jiang and C. Wang, *J. Alloys Comp*., **509**, 5336 (2011).